Flow Over an Inclined Plate[1]

F. H. ABERNATHY
Assistant Professor, Division of Engineering and Applied Physics, Harvard University, Cambridge, Mass. Assoc. Mem. ASME

A free-streamline theory for an inclined flat plate in an infinite flow field, at an arbitrary angle of attack, is presented. Measurements of the location of the free-vortex layers, of the vortex-street frequency, and of the pressure behind an inclined sharp-edge plate are reported as a function of both the angle of attack of the plate and the lateral constriction of the flow. The separation between free-vortex layers is found experimentally to be essentially independent of lateral flow constriction. A form of the Strouhal number, using this separation distance as the characteristic flow dimension, is shown to be independent of lateral constriction of the flow and of the inclination of the plate.

Introduction

THREE distinct flow patterns characterize the flow of a fluid over an infinite flat plate or airfoil inclined to the direction of the undisturbed flow: streamlined-body flow at low angles of attack, transitional or stalling flow at moderate incidences, and bluff-body flow at intermediate and at high incidences. While the first two types of flow have been investigated intensively because of their importance to aeronautics, bluff-body flow has received comparatively little attention.

Although the essential features of bluff-body flow have been known for many years, it cannot yet be described in detail. Consider for example an infinite flat plate inclined at an angle of attack α to the main stream flow direction. In the incidence range from approximately 30 to 90 deg, the fluid flowing from the stagnation point toward the leading and trailing edges is unable to turn around the edges and separates permanently from the plate at both points. The separation of the flow at both the leading and trailing edges gives rise to a region of constant low static pressure over the entire upper surface of the plate. The separated or free-boundary layers (which would be more accurately termed free-vortex layers) are unstable and, through an interaction not yet understood, are partially transformed into a vortex street in the wake.

Kirchhoff's classical free-streamline theory for flow normal to a flat plate [1][2] attempts to predict mean pressure drag of such a plate by assuming that a streamline of the flow, on which the flow speed is equal to the magnitude free-stream velocity U_0, originates at the edges of the plate. These free streamlines separate the outer potential flow from the assumed stagnant wake behind the body in which the pressure is assumed to be equal to the free-stream static pressure p_0. Rayleigh [1] extended Kirchhoff's free-streamline theory to include a plate at an arbitrary inclination to the main stream.

While this classical free-streamline theory does describe some of the general features of the mean flow such as the free-vortex layer and the constant pressure behind the plate, it is unrealistic in specific detail. The classical theory of Kirchhoff-Rayleigh predicts a drag coefficient of $2\pi \sin \alpha/(4 + \pi \sin \alpha)$ for a plate inclined at an angle α to the main stream. For a normal plate this reduces to 0.88, while Flachsbart [2] measured a value of 1.96 which was independent of the flow Reynolds number from 6×10^3 to at least 6×10^5. This discrepancy between theory and experiment was explained by Fage and Johansen [3] who observed experimentally that the maximum mean velocity U_s in the free-

[1] This paper is based on part of a thesis submitted to Harvard University in partial fulfillment of the requirements for the PhD degree in Engineering.

Contributed by the Fluid Meters Subcommittee of the Hydraulic Division and presented at the Winter Annual Meeting, New York, N. Y., November 26–December 1, 1961, of THE AMERICAN SOCIETY OF MECHANICAL ENGINEERS. Manuscript received at ASME Headquarters, July 28, 1961. Paper No. 61—WA-124.

[2] Numbers in brackets designate References at end of paper.

Nomenclature

a = stagnation point on plate
b = upper edge of plate; b' lower edge of plate
C_p = local pressure coefficient, $(p - p_0)/{}^1/_2\rho U_0^2$
$C_p{}^*$ = pressure coefficient behind plate, $(p_s - p_0)/{}^1/_2\rho U_0^2$
c = plate chord
D = separation distance between free streamlines
d = point on upper free streamline; d', point on lower free streamline
$F(\phi)$, $f(\phi)$, $G(\phi)$, $H(\phi)$ = functions used to simplify writing and defined in text
g, h = co-ordinates of I in η-plane
I = point at infinity in z-plane
K = dimensionless constriction ratio, L/c
k = velocity ratio, U_s/U_0
L = height of tunnel test section
l = a constant, t/h
m = a constant, $t^2(1 - g^2)h^2$
n = predominant frequency in wake
p = local static pressure; p_0, free-stream static pressure; p_s, static pressure behind plate in bluff-body flow
q = magnitude of velocity, $|v|$
R = $|I_\zeta|$
$\mathbf{R}$ = dimensionless flow Reynolds number, $U_0 c\rho/\mu$
$\mathbf{S}$ = dimensionless conventional Strouhal number, $nc \sin \alpha/U_0$
$\mathbf{S}^*$ = dimensionless modified Strouhal number, nD/U_s
t^2 = a constant, $h^2/[h^2 + (1 - g)^2]$
U = local velocity; U_0, free-stream speed and average speed across test section; U_s, maximum speed on free streamlines or in free-vortex layers
u, v = x and y-components of velocity, respectively
w = complex potential, $\phi + i\psi$
x, y = co-ordinates in physical plane
z = complex variable, $x + iy$
α = angle of attack
β = a constant, $2g/(g^2 + h^2 + 1)$
ζ = a complex variable, $1/\nu$
η = a complex variable, $i[\zeta - 1/\zeta]/2$
μ = viscosity
ν = complex conjugate velocity, $u - iv$
τ = a complex variable
ϕ = scalar potential
ψ = scalar stream function
ρ = fluid density, a constant

vortex layers issuing from an inclined plate was considerably greater than the free-stream velocity U_0, and that the pressure behind the body was less than the free-stream pressure p_0 assumed in the classical theory. They showed, in fact, that the observed drag coefficient on an inclined plate was very nearly given by $(U_s/U_0)^2$ times the value predicted from the Kirchhoff-Rayleigh theory.

Roshko [4, 5] modified the classical free-streamline theory for the cases of the normal flat plate, circular cylinder, and 90-deg wedge by assuming the flow speed on the separated free-streamlines to be a constant k times U_0. The drag coefficient predicted by this modified theory for the normal flat plate agrees quite well with the value measured by Fage and Johansen [3], provided the experimentally measured value of k is used in the theory. This modified theory also predicts a finite separation between the free-streamlines for all values of k greater than one, and reduces to the classical theory when k is equal to unity. Using this calculated separation distance as the characteristic flow dimension for each of the three bluff bodies in conjunction with the measured value of U_s and the Karman vortex-street frequency in the wake, Roshko [6] was able to formulate a modified Strouhal number which was nearly the same for all three bluff bodies.

This paper is concerned with the elaboration of the modified free-streamline theory to include a plate at an arbitrary angle of attack, and with an experimental investigation of the behavior of the flow field in the vicinity of an inclined plate in a constricting flow channel.

Free-Streamline Theory for an Inclined Plate

Analytical Model. Free-streamline theory represents an attempt to describe the mean flow of a real fluid in the immediate vicinity of a bluff body by using a steady potential-flow model. The theory does predict a wake extending to infinity behind the body, and it does not consider the instability of the vortex sheets emanating from the bluff body. Both of these features are unrealistic. Regarding the infinite wake, Batchelor [7] has pointed out that although free-streamline theory might be the appropriate mathematical solution for the case of a fluid with identically zero viscosity, the more likely solution for a real fluid at high Reynolds number would probably have a closed wake, ending in a cusp, with the two standing vortexes inside the wake. The free-streamlines, which are idealizations of the free-vortex layers, are clearly unstable, and in a real fluid give rise to a moving vortex street some distance downstream in the wake of a bluff body (in the appropriate Reynolds number range). The modified free-streamline theory being presented in this paper can only be expected to represent the mean flow conditions near an inclined plate.

The assumed two-dimensional, free-streamline flow of a nonviscous, incompressible fluid over a plate inclined at an angle α to the stream direction is sketched in the z-plane of Fig. 1. The boundaries of the potential-flow field are formed by one streamline which bifurcates at the stagnation point a, on the forward surface of the plate. The upper branch of this streamline separates from the plate at the upper edge b, and the lower branch separates from the plate at the lower edge b'. It will be assumed that the fluid speed U_s on the free streamline from b to d and from b' to d' is constant and equal to kU_0, with k arbitrary though greater than one. The essential features of the mean flow in the vicinity of the inclined plate have been specified; the speed U_s on the free streamlines is constant and greater than U_0, and a uniform pressure determined by U_s exists behind the plate.

The problem is to determine the location of the boundaries of the flow (the dividing streamline) in the z-plane and to calculate the velocity distribution on the front surface of the plane. This dividing streamline, on which the stream function ψ is necessarily

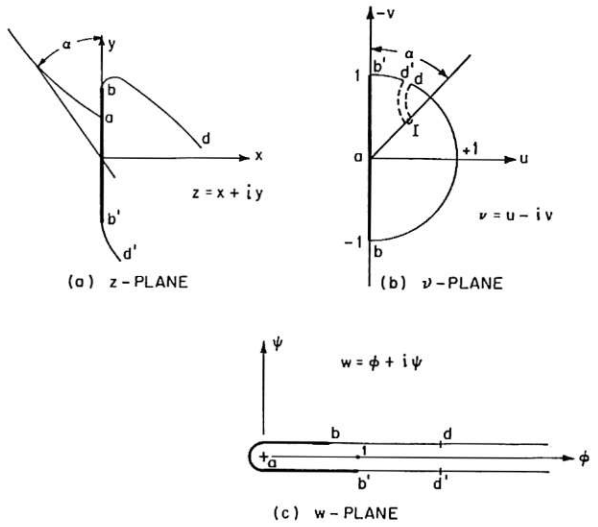

Fig. 1 Sketch of flow boundaries in: (a) Physical plane, (b) hodograph plane, and (c) complex potential plane

constant and for convenience is taken to be zero, is shown in the plane of the complex potential $w = \phi + i\psi$ in Fig. 1.

The z-plane and w-plane are related to each other through the complex hodograph, the plane of the complex conjugate velocity v.

$$v = u - iv = \frac{1}{\zeta} = \frac{dw}{dz} = \frac{d\phi}{dx} + i\frac{d\psi}{dx}, \qquad (1)$$

$z = x + iy$; u and v are the components of the velocity in the x and y-directions, respectively. Therefore, if the v-plane, or its inverse the ζ-plane, can be mapped into the w-plane, the position of the free streamlines can be determined by integration of equation (1) along the contour formed by the boundaries of the flow field in the w-plane, that is

$$z = \int \zeta(w)dw + \text{constant} \qquad (2)$$

In the classical theory of Kirchhoff-Rayleigh the boundaries of the flow form a semicircle in the v-plane. The speed on the free streamlines is assumed constant and equal to U_0; hence the equation of the free streamlines off the plate is simply $|v| = U_0$ with $u > 0$, or a semicircle in the hodograph. On the plate $u = 0$ and $-U_0 \leq v \leq U_0$, therefore this portion of the flow boundary in the hodograph closes the semicircle along the vertical diameter. The flow velocity at infinity in the z-plane is U_0 and the pressure is p_0; in other words, free-stream conditions exist at large distances before and behind the plate outside of the wake.

The hodograph for this modified free-streamline flow, Fig. 1, is similar to that of the classical theory. The speed on the free streamlines from b to d and b' to d' is constant and equal to kU_0; therefore in the hodograph this portion of the flow boundary must again lie on a circular arc. At great distances downstream of the plate, the flow on the free streamlines should attain free-stream conditions; therefore the point at infinity cannot lie on the circular arc in this hodograph but must be inside the circle. Roshko [4], in discussing the normal plate, reasoned that the flow near the plate cannot be influenced greatly by the deceleration on the free streamline, provided the transition occurs after a region of constant flow speed. He therefore suggested a radial cut (for the normal plate) inward from the circular arc to the point corresponding to infinity. The boundaries of this cut were perpendicular to the plate, hence on the cut or notch the flow was parallel to the main stream direction. This implied a maximum distance between free streamlines.

In the case of the inclined plate, a radial notch in the hodograph presents mathematical difficulties in mapping the hodograph onto the w-plane. In order to simplify the mathematical transformations, the more complicated geometrical notch in the ν-plane of Fig. 1 is suggested. At the beginning of the cut, the flow is not in the direction of the free stream; that is, a line joining d' to d in the z-plane will not be perpendicular to the undisturbed flow. The length of this line then cannot be used as a characteristic dimension of the wake; however, it will be shown later that the location of the streamlines up to the points d and d' predicted by the theory is in excellent agreement with experiment for laterally unrestricted flow.

Mathematical Solution. All of the planes needed to map the ν-plane onto the w-plane are sketched in Fig. 2. For convenience the maximum speed kU_0 on the free streamlines has been taken to be unity, which requires that $|a - b'| = k|a - I|$ to preserve the scale. The potential ϕ has been set equal to unity at the lower separation point b'; its value at the upper separation point b must be determined from the calculations.

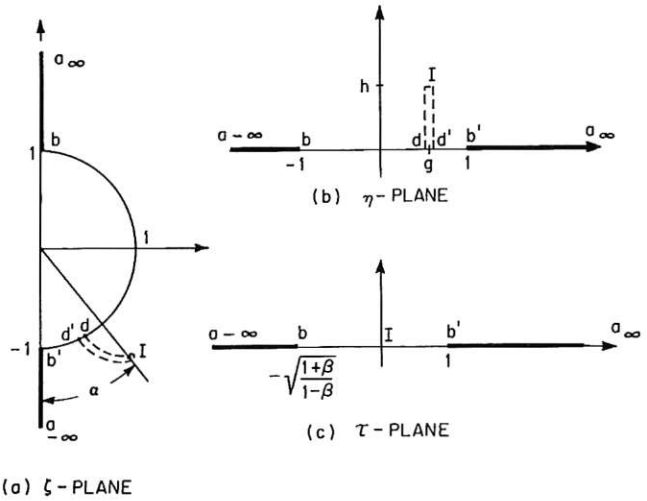

Fig. 2 Sketch of flow boundaries in three intermediate complex planes

The form of the desired over-all mapping function is easily obtained by performing several intermediate steps. With the ν-plane as the starting point, the ζ-plane is obtained by a simple inversion. The η-plane is obtained from the ζ-plane by the Joukowsky type of transformation that is so common in airfoil theory:

$$\eta = i/2\left[\zeta - \frac{1}{\zeta}\right] \tag{3}$$

The "notched" portion of the hodograph, d-I-d', has now been transformed into a vertical cut in the η-plane. The exact shape of the notch in the ν-plane can of course be determined; however, it is not important for the development. One need only require that the notch in the η-plane be a vertical cut.

The mapping of the η-plane onto the w-plane involves the straightforward, intermediate transformations sketched in Fig. 2. The function

$$\tau^2 = \frac{(\eta - g)^2 + h^2}{(1 - g)^2 + h^2} \tag{4}$$

maps the η-plane onto the τ-plane. The transformation from the τ-plane to the w-plane is

$$w = 1/\tau^2 \tag{5}$$

The over-all mapping function $\zeta(w)$, formed by combining equations (3, 4, and 5), is

$$\zeta(w) = -\frac{ih}{t}\left\{\pm\sqrt{\frac{1}{w} - t^2} + \frac{gt}{h} \mp \sqrt{\frac{1}{w} - t^2 \pm \frac{2gt}{h}\sqrt{\frac{1}{w} - t^2} - \frac{t^2}{h^2}(1 - g^2)}\right\} \tag{6}$$

with $t^2 = h^2/[h^2 + (1 - g)^2]$. The flow speed ($q$) along the dividing streamline can be obtained directly by evaluating equation (6) as a function of ϕ along the boundary $\phi = 0$ in the w-plane, since $q = |\nu| = |1/\zeta|$. The correspondence between z and ϕ is established through equation (2). The correct branch of ζ, the relation between z and ϕ, and the limits of ϕ on the relevant portions of the dividing streamline follow:

On the plate between a and b

$$\zeta = i/l\left\{f - gl + \sqrt{f^2 - 2glf - m}\right\}, \tag{7a}$$

$$z = i/l\{F(\phi) - gl\phi + G(\phi)\}, \tag{7b}$$

with

$$0 \leq \phi \leq \phi_1; \tag{7c}$$

along the separated streamline from b to d,

$$\zeta = i/l\left\{f - gl - i\sqrt{|f^2 - 2glf - m|}\right\} \tag{8a}$$

$$z = i/l\{F(\phi) - gl\phi + F(\phi_1) - i[F(\phi) - F(\phi_1)]\} \tag{8b}$$

with

$$\phi_1 \leq \phi \leq \phi_2; \tag{8c}$$

on the plate between a and b';

$$\zeta = -i/l\left\{+f + gl + \sqrt{f^2 + 2glf - m}\right\}, \tag{9a}$$

$$z = -i/l\{F(\phi) + gl\phi + H(\phi)\}, \tag{9b}$$

with

$$0 \leq \phi \leq \phi_3; \tag{9c}$$

along the separated streamline from b to d',

$$\zeta = -i/l\left\{f + gl + i\sqrt{|f^2 + 2glf - m|}\right\}, \tag{10a}$$

$$z = -i/l\{F(\phi) + gl\phi + H(\phi_3) + i[H(\phi) - H(\phi_3)]\} \tag{10b}$$

with

$$\phi_3 \leq \phi \leq \phi_4; \tag{10c}$$

where

$$\phi_1 = \frac{1 - \beta}{1 + \beta}, \qquad \phi_2 = 1/t^2$$

$$\phi_3 = 1, \quad \phi_4 = 1/t^2,$$

$$f(\phi) = \sqrt{\frac{1}{\phi} - t^2}, \quad F(\phi) = \int_0^\phi f(\phi')d\phi' = \sqrt{\phi(1 - t^2\phi)} + \frac{1}{t}\tan^{-1}\sqrt{\frac{t^2\phi}{1 - t^2\phi}},$$

$$G(\phi) = \int_0^\phi \sqrt{|f^2(\phi') - 2glf(\phi') - m|}\, d\phi',$$

$$H(\phi) = \int_0^\phi \sqrt{|f^2(\phi') + 2glf(\phi') - m|}\, d\phi',$$

$$l = t/h, \quad m = t^2(1 - g^2)/h^2, \quad \text{and } \beta = \frac{2g}{g^2 + h^2 + 1}.$$

The specific forms for $G(\phi)$ and $H(\phi)$ are rather involved, and for actual calculations it was found easier to carry out the integrations numerically since $\zeta(\phi)$ must be evaluated in order to calculate the pressure distribution.

Before the integrations can be carried out for a specific case, the parameters g and h (which appear in the equations for ζ and z and in the limits for ϕ), must be related to the angle of attack α and the velocity ratio k. Referring to Fig. 2, the co-ordinates of the point at infinity, I, in the ζ-plane can be represented in polar form as $I_\zeta = \mathrm{Re}^{i\theta}$. The transformation to the η-plane is given by equation (3); therefore the co-ordinates of I in the η-plane expressed in terms of I_ζ are

$$I_\eta = g + ih = -\frac{\sin\theta}{2}\left[R + \frac{1}{R}\right] + i\frac{\cos\theta}{2}\left[R - \frac{1}{R}\right] \quad (11)$$

The angle $\theta = -\pi/2 + \alpha$ and the modulus of I_ζ is k, hence

$$g = \frac{\cos\alpha}{2}\left[k + \frac{1}{k}\right], \quad \text{and} \quad h = \frac{\sin\alpha}{2}\left[k - \frac{1}{k}\right] \quad (12)$$

In the hodograph, the speed at infinity is $1/k$ and the local speed is $|\nu|$ or $|1/\zeta|$; therefore the local pressure coefficient C_p is simply

$$C_p = \frac{p - p_0}{\frac{1}{2}\rho U_0^2} = 1 - \left(\frac{U}{U_0}\right)^2 = 1 - \frac{k^2}{|\zeta|^2} \quad (13)$$

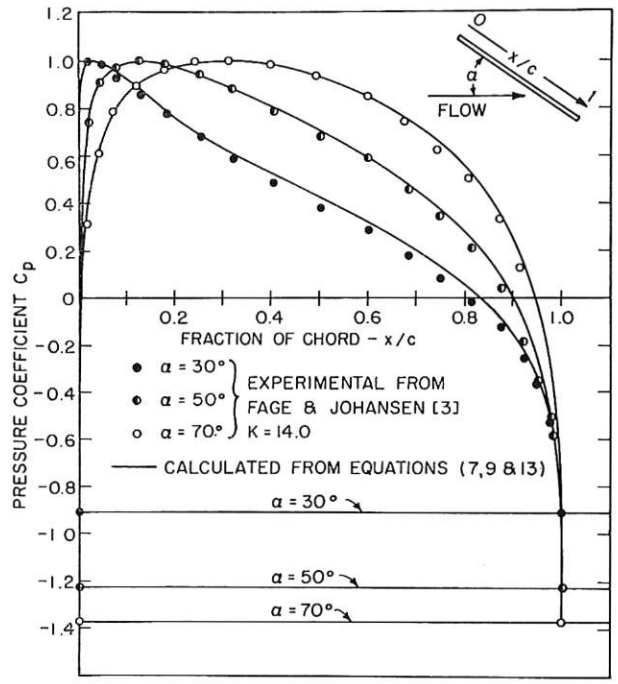

Fig. 3 Calculated and experiment pressure coefficients on an inclined sharp-edged plate for $K = 14$

The pressure distribution on the front surface of a flat plate at three different incidences has been calculated from this modified free-streamline theory, using Fage and Johansen's [3] experimentally measured values of k, and the results are presented in Fig. 3. In general, the theoretical results appear to predict adequately the mean flow distribution, and therefore the lift and drag on an inclined plate in an infinite flow field, provided k has been determined experimentally.

The location of the free streamlines was calculated from the foregoing theory for a plate inclined at 40 deg and compared with

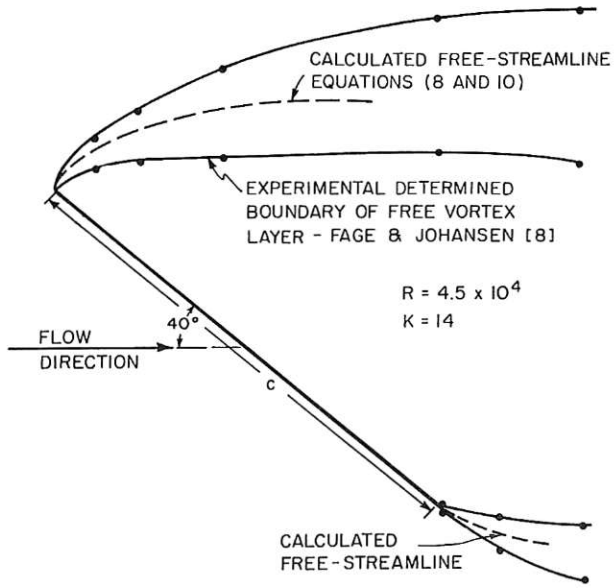

Fig. 4 Location of free-vortex layers and calculated free streamlines from a sharp-edged plate with $\alpha = 40$ deg and $K = 14$

the experimental results of Fage and Johansen [8]. From Fig. 4, one can see that the theoretical results just about fall on the center line of the experimentally measured boundaries of the free-vortex layers. Part of the width of the layers is due to the diffusion of vorticity, and part is due to the oscillation of the layers caused by the vortex street farther downstream in the wake.

Experimental Investigation

Apparatus. The modified free-streamline theory for the inclined plate appears to be adequate to describe the mean flow at least when the lateral constriction of the flow is not too great. (The quoted results of Fage and Johansen are for a tunnel height to plate chord ratio of 14.) An experimental investigation was undertaken to determine what effect lateral constriction of the flow has on the applicability of the free-streamline theory, and in order to determine the location of the free-vortex layers from an inclined plate as a function of inclination and lateral constriction of the flow.

For this purpose a small (7 by 3-in. test section), single-pass, air-suction tunnel was constructed. The tunnel, associated constant current hot-wire equipment, and calibration procedures are described in detail in [9]. Five different flat-plate models were used in the experiments. The relevant physical dimensions of the plates are presented in Table 1. All of the plates, except for the one with rounded edges, were trapezoidal with equal included angles at the leading and trailing edges.

Table 1 Dimensions of flow models

Model chord, c, in.	Angle at leading and trailing edges, deg	Thickness, in.	Tunnel height, chord K
1.991	22.5	0.125	3.51
1.349	Hand rounded	0.125	5.18
1.326	22.5	0.125	5.27
1.000	25.0	0.125	6.99
0.500	25.0	0.094	13.98

The plates were supported horizontally and completely spanned the 3-in. width of the test section. The horizontal axis through the plates at the mid-chord and mid-thickness point was fixed along the center line of the test section by pins through the transparent vertical walls. The span of the plates was just slightly larger than the width of the test section. Hence to adjust

the angle of attack of a plate, it was necessary to loosen a side wall which, when tightened, held the model firmly at its preset incidence. Through careful machining it was possible to maintain sufficient compression in the models to prevent their rotation under flow conditions without buckling. This method of support prevented end leakage which can have a pronounced influence on the static pressure behind the model [2] and on the frequency of the vortex street in the wake.

A constant-current, hot-wire anemometer was used to determine the boundaries of the free-vortex layer and to measure the frequency of the vortex street in the wake behind the plates. Since the region between the separated vortex layers is important to the general flow field [6], the traversing hot-wire probe was supported well downstream of the flow models (more than 7 in.) and was designed [9] to allow traversing of the separated flow while keeping the main portion of the probe parallel to the tunnel

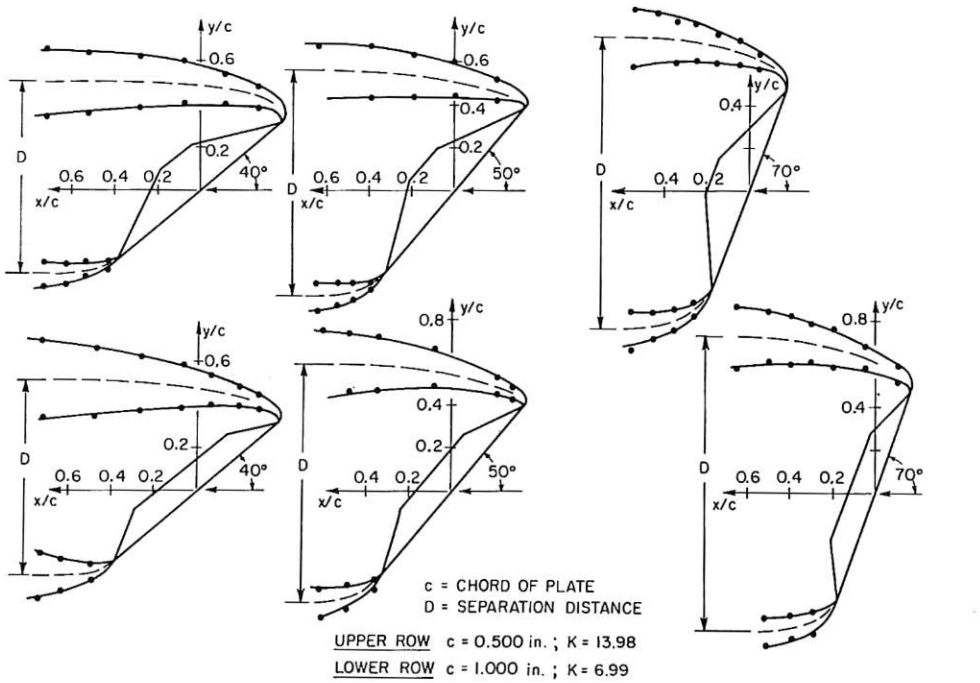

Fig. 5 Free-vortex layers from inclined sharp-edged plates with lateral flow constriction: $K = 13.98$ and 6.99

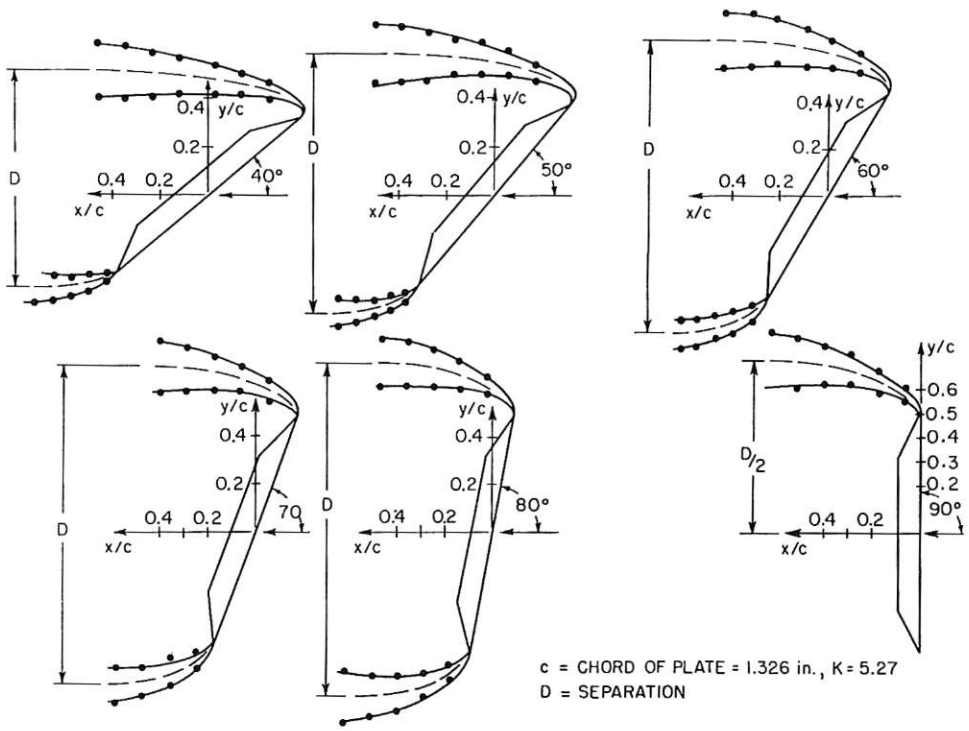

Fig. 6 Free-vortex layers from an inclined sharp-edged plate with lateral flow constriction: $K = 5.27$

axis outside of the wake. The sensing end of the instrument, inclined at 60 deg to the body of the probe, supported the hot wire between $^3/_4$-in-long needles. The traversing mechanism, which permitted two translational degrees of freedom, was housed in a sealed space adjacent to the tunnel.

Location of Free-Vortex Layers. The boundaries of the free-vortex layers were determined from velocity traverses across the layers normal to the tunnel axis. The outer and inner boundaries of the free-vortex layers, at any downstream station, were taken to be the points of maximum and minimum mean velocity along the traverse [3, 8]. Near the edges of the plates the boundaries of the layers were quite distinct, while farther downstream the boundaries become much less well defined. In all cases of the plates investigated, it was possible to distinguish these boundaries of the free-vortex layer sufficiently far downstream in the wake for the layers to become parallel.

The location of the outer and inner boundaries of the free-vortex layers emanating from the leading and trailing edges of three flat plates of different chord length at varying incidences is shown in Figs. 5 and 6. The solid circles are the points of either maximum or minimum mean velocity. The broken line is simply the locus of points midway between the outer and inner boundaries of the free-vortex layers and has been taken to be representative of the location of the free streamline, Fig. 4. The length D shown in Figs. 5 and 6 is simply the distance, measured perpendicularly to the free-stream direction, between the median lines in both free-vortex layers where the two median lines have become parallel. This length D has been taken to be a reasonable measure of the separation between free-vortex layers; it will be simply referred to as the separation distance. All of the experimental data were taken with the average air speed across the test section maintained at 140 fps. The results of the measurements of the separation distance are presented in Table 2. The location of the free-vortex layers for the three plates at the same incidence is shown in collected form in Fig. 7 for three different values of α.

Table 2 Separation of free streamlines

Model chord, c, in.	Angle of attack, α, deg	Separation of free streamlines — D/c, chord lengths	Separation of free streamlines — $D(c \sin \alpha)$, projected chord lengths
1.326	40	0.895	1.390
1.326	50	1.075	1.403
1.326	60	1.210	1.397
1.326	70	1.325	1.410
1.326	80	1.390	1.415
1.326	90	1.430	1.430
1.000	40	0.900	1.398
1.000	50	1.100	1.435
1.000	70	1.355	1.437
0.500	40	0.900	1.398
0.500	50	1.065	1.390
0.500	70	1.355	1.437

NOTE: Average value of $D/(c \sin \alpha) = 1.412$.
Standard deviation of values of $D/(c \sin \alpha) = 0.018 = 1.3$ per cent mean value of $D/(c \sin \alpha)$.

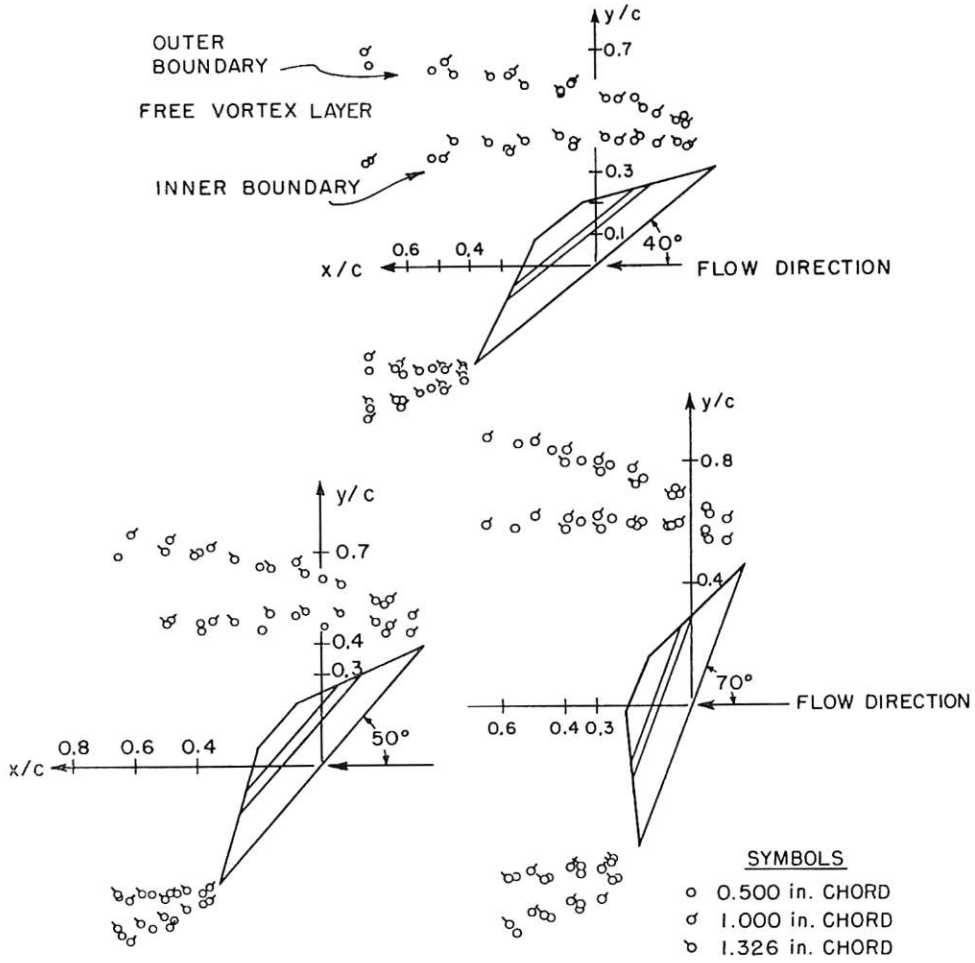

Fig. 7 Comparison of location of free-vortex layers from inclined sharp-edged plates at three angles of attack with varying lateral flow constriction

It is apparent from Fig. 7 and Table 2 that the separation distance is essentially independent of the constriction ratio K from at least 14 to 5.27, and is approximately equal to $\sqrt{2}\, c \sin \alpha$. This result is quite surprising. It suggests that over a wide range of lateral constriction the characteristic flow dimension for an inclined sharp edged, flat plate in bluff-body flow is $\sqrt{2}$ times the length of the chord projected normal to the flow. If this length is the characteristic dimension of the flow even in a relatively constricted-flow channel, then a modified Strouhal number based on this length on the frequency of the vortex street in the wake, and on the maximum mean speed in the separated vortex layers, should be independent of the constriction ratio K and the angle of attack α.

Vortex-Street Frequency. In order to calculate the proposed modified Strouhal number it was necessary to determine experimentally both the frequency n of the vortex street behind the plates and the maximum mean speed U_s in the separated vortex layers.

The predominant frequency n of the vortex street was determined from hot-wire anemometer data. Since the frequency was quite pronounced, it was possible to determine it directly from Lissajous' figures of the hot-wire response projected on an oscilloscope. The value of n obtained by this method was checked by comparing the hot-wire response with a known frequency signal on a dual-beam oscilloscope. Most of the frequency data were obtained with the sensing element of the traversing probe located outside of the wake, a chord length or more behind the leading edge. The frequency measured at this point was checked by simultaneously measuring the frequency with another probe inserted into the working section through the upper wall of the tunnel, and it was found to be independent of the position of the probe.

Table 3 Measured vortex-street frequencies in cycles per second behind flat plates

Angle of attack	Model chord, in.					
	1.991[a]	1.349[a,c]	1.326[a]	1.000[a]	1.000[b]	0.500[a]
α, deg	n	n	n	n	n	n
90	206	261	251	300	150	540
85	206	261	251	304	155	541
80	207	265	251	306	157	551
75	207	269	255	311	156	563
70	210	275	259	319	159	577
65	211	282	263	327	166	602
60	213	285	268	339	171	632
55	214	293	281	363	176	673
50	222	309	291	373	189	723
45	231	332	306	407	199	794
40	250	353	325	442	222	869
35	275	390	355	484	249	979
30	312	448	396	585	294	1105

[a] Measured at $U_0 = 140$ fps.
[b] Measured at $U_0 = 70$ fps.
[c] Rounded leading and trailing edges.

The results of the experimental determination of the vortex-street frequency n are summarized in Table 3. Since it was already known that the drag of a plate in bluff-body flow is independent of the flow Reynolds number $\mathbf{R}$ from $\mathbf{R} = 6 \times 10^3$ to at least $\mathbf{R} = 6 \times 10^5$ [2], it was suspected that n would be directly proportional to U_0 within this range of $\mathbf{R}$. The vortex-street frequency behind the 1-in. chord plate was measured throughout the range of α at both U_0 equal to 140 and 70 fps. From Table 3 it can be seen that n is essentially proportional to U_0 for the 1-in. plate; therefore the Reynolds-number dependence of n need not be considered.

Static Pressure Behind Plates. The maximum mean speed U_s in the free-vortex layers from the inclined plates was calculated from measurements of the static pressure on the rear surface of the plates. Fage and Johansen [3], and Rose and Altman [10] have shown that sharp-edged plates stall by separation of the boundary layer from the leading edge, followed by reattachment of the flow downstream of the leading edge with the point of reattachment moving rearward as the angle of attack increases. The static pressure between the leading edge and the point of reattachment is essentially constant, and once complete separation has occurred (bluff-body flow) the static pressure over the entire upper surface is constant and relatively independent of the shape of the upper surface. Therefore it is only necessary to measure the pressure at one point on the rear surface of the plate to obtain a representative value.

For convenience the pressure behind the plates (p_s) was measured at a small orifice located at mid-chord and mid-span of each model. From this measurement, the pressure coefficient behind the plates $C_p{}^*$ was computed. The maximum mean speed U_s in the free-vortex layers was determined from $C_p{}^*$ by assuming the fluid between the layers to be stagnant and by applying Bernoulli's theorem; that is,

$$\frac{p_s - p_0}{{}^1/_2 \rho U_0{}^2} = C_p{}^* = 1 - \left(\frac{U_s}{U_0}\right)^2 = 1 - k^2 \qquad (14)$$

Fage and Johansen [3] have shown that the maximum mean speed estimated from the pressure coefficient behind the plate agrees quite well with direct measurements of the maximum speed in the vortex sheets near the plate.

The flow conditions for the static-pressure measurements behind all of the models listed in Table 1 were the same as those used to measure the frequency of the vortex street. The results of the pressure measurements are presented in Table 4 and Fig. 8. The measurements of Fage and Johansen [3] which correspond to a constriction ratio of 14 are plotted in Fig. 8 along with the results of this investigation for the same value of K. The agreement between these two sets of measurements is fairly poor. The difference between them represents the effect of the clearance be-

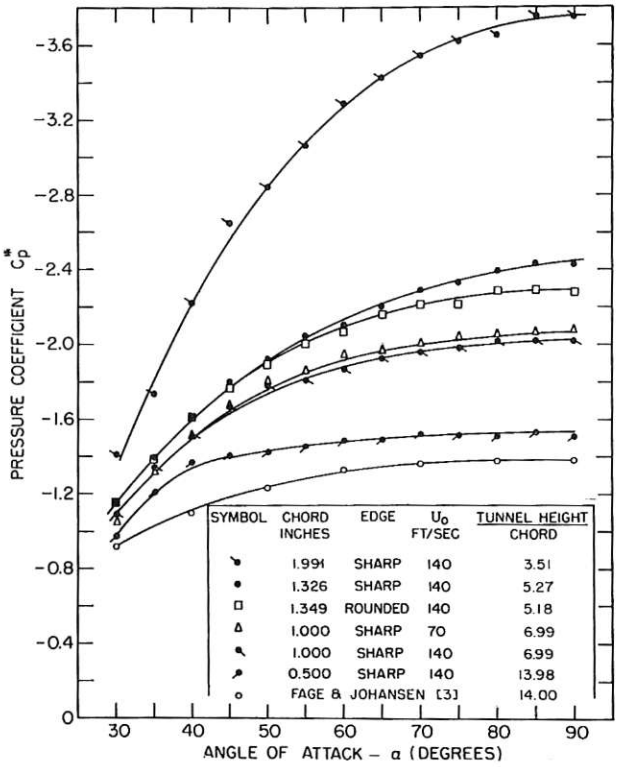

Fig. 8 Pressure coefficient behind inclined flat plates with varying lateral flow constriction

tween the plate and the tunnel walls in the experiments of Fage and Johansen. The drag coefficient for a normal flat plate with $K = 14$ was reported in [3] to be 2.13, and for $K = \infty$ the drag was estimated to be 1.84. Flachsbart [2] on the other hand reported a value of 1.96 for $K = \infty$ with the plate sealed to the side walls of the tunnel. To a first approximation, the ratio of these two values of drag for $K = \infty$ is simply the ratio of the square of U_s for these two cases. Fage and Johansen's value [3] of $C_p{}^*$ for $\alpha = 90$ deg can be corrected for end leakage by using this ratio of drag coefficients and equation (14). When this correction is applied, the value of $C_p{}^*$ in [3] becomes -1.55 which agrees quite well with the value of -1.50 reported in this investigation.

Correlation of Frequency, Velocity, and Free-Streamline Separation

Using the experimental values of the vortex-street frequency, of the maximum mean speed in the separated vortex layer, and of the separation distance, it is possible to formulate a modified Strouhal number S^* defined as,

$$\mathsf{S}^* = \frac{nD}{U_s} = \frac{n\ 1.41\ c \sin\alpha}{kU_0} = \frac{n\ 1.41\ c \sin\alpha}{\sqrt{1 - C_p{}^*}\,U_0}, \qquad (15)$$

Which is essentially independent of both the flow constriction and angle of attack for the sharp-edged plates. This modified Strouhal number S^* is similar to the one proposed by Roshko [4]; the difference lies in the definition of the separation distance D. Roshko used a theoretically determined separation distance which was a function of k and was valid only for unrestricted flow. The modified Strouhal number proposed here for sharp-edged flat plates uses an empirical value for the separation distance which appears to be essentially independent of the flow constriction.

Both the conventional Strouhal number S (defined as $nc \sin\alpha/U_0$) and S^* have been calculated for all of the flat plates in Table 1 and are listed in Table 5. The value of S^* is essentially constant for each plate over the range of α from approximately 35 to 90 deg. In addition, the mean value of S^* over this range of α is roughly the same for all of the sharp-edged plates. The average values of the Strouhal numbers for the various plates are summarized in Table 6. The mean value of S^* varies from 0.147 to only 0.153 for the sharp-edged plates over the range of $\alpha = 35$ to 90 deg, while over the same range of α the mean value of S varies from 0.164 to 0.219. For the sharp-edged plates, the proposed modified Strouhal number S^* is essentially independent of the angle of attack (provided bluff-body flow is well established) and of the lateral constriction of the flow; while the conventional Strouhal number S varies considerably with both α and K.

The separation distance D in equation (15) was measured for sharp-edged plates for values of K between 5.27 and 13.98 and for $\alpha \geq 40$ deg. From the data in Table 5 it is clear that the proposed S^* correlation can be extended to $K = 3.51$ (the 1.991-in-chord plate) without greatly changing the values of S^* from those for larger values of K. Values of S and S^* for $\alpha = 30$ and 35 deg are included in Table 5 because a vortex frequency was observed; however, it is seen that S^* at $\alpha = 30$ deg is considerably greater than either its mean value over α or its value at $\alpha = 35$ deg. This variation in S^* is due to incomplete separation of flow at the lower angle of attack. The leading and trailing-edge angle of the plates was 25 deg for the two smallest models and 22.5 deg for the two largest sharp-edged plates. Hence at $\alpha = 30$, the angle between the undisturbed flow direction and the upper surface of the plate was only 5 or 7.5 deg. This would suggest that complete separation had not occurred and the D might well be less than $\sqrt{2} \sin\alpha$ and S^* consequently greater than its mean value.

The mean value of S^* for the 1.349-in-chord plate (rounded edges rather than sharp edges) in Table 6 is 0.162 which is considerably greater than the mean S^* for the sharp-edged plates. Since S^* for this model was nearly a constant independent of α, it suggested that the appropriate value of D in equation (15) should not have been $\sqrt{2} \sin\alpha$ if S^* were to be the same for both rounded and sharp-edged plates, but rather 1.3 sin α. While no detailed experimental measurements of D for the rounded-edge plate were made, it was verified at one value of α that D was indeed smaller for the rounded-edge plate than for the sharp-edged plate.

Table 4 Measured pressure coefficients, C_p, behind inclined flat plates

Angle of attack, α, deg	Model, chord, in. 1.991[a] $-C_p{}^*$	1.349[a,c] $-C_p{}^*$	1.326[a] $-C_p{}^*$	1.000[a] $-C_p{}^*$	1.000[b] $-C_p{}^*$	0.500[a] $-C_p{}^*$
90	3.75	2.28	2.42	2.02	2.05	1.50
85	3.77	2.29	2.43	2.01	2.04	1.53
80	3.65	2.28	2.39	2.01	2.05	1.51
75	3.62	2.22	2.33	1.98	2.04	1.51
70	3.54	2.20	2.28	1.96	2.00	1.52
65	3.42	2.16	2.21	1.92	1.96	1.49
60	3.29	2.07	2.10	1.86	1.94	1.49
55	3.07	2.01	2.05	1.80	1.86	1.45
50	2.84	1.89	1.92	1.78	1.81	1.42
45	2.65	1.78	1.80	1.66	1.69	1.40
40	2.22	1.61	1.61	1.51	1.51	1.37
35	1.74	1.40	1.39	1.35	1.33	1.22
30	1.41	1.18	1.15	1.09	1.04	0.98

[a] Measured at $U_0 = 140$ fps.
[b] Measured at $U_0 = 70$ fps.
[c] Rounded leading and trailing edges.

Table 5 Strouhal numbers computed from experimental data for inclined flat plates

Angle of attack, α, deg	$c = 1.991$[a] in. ($K = 3.51$) S^*	S	$c = 1.349$[a,c] in. ($K = 5.18$) S^*	S	$c = 1.326$[a] in. ($K = 5.27$) S^*	S	$c = 1.000$[a] in. ($K = 6.99$) S^*	S	$c = 1.000$[b] in. ($K = 6.99$) S^*	S	$c = 0.500$[a] in. ($K = 13.98$) S^*	S
90	0.158	0.244	0.163	0.210	0.151	0.198	0.145	0.179	0.144	0.179	0.144	0.161
85	0.157	0.243	0.163	0.209	0.150	0.197	0.147	0.180	0.148	0.183	0.143	0.161
80	0.159	0.242	0.163	0.210	0.149	0.195	0.146	0.179	0.149	0.185	0.145	0.163
75	0.156	0.237	0.163	0.209	0.150	0.194	0.146	0.179	0.146	0.180	0.145	0.163
70	0.155	0.233	0.163	0.207	0.149	0.192	0.146	0.178	0.144	0.177	0.144	0.162
65	0.152	0.226	0.163	0.206	0.148	0.188	0.146	0.176	0.147	0.179	0.147	0.163
60	0.149	0.218	0.160	0.198	0.146	0.183	0.146	0.175	0.145	0.176	0.146	0.164
55	0.145	0.207	0.157	0.193	0.147	0.182	0.149	0.177	0.143	0.171	0.144	0.164
50	0.145	0.201	0.158	0.191	0.145	0.176	0.144	0.170	0.145	0.173	0.150	0.165
45	0.143	0.193	0.160	0.189	0.143	0.170	0.148	0.171	0.143	0.167	0.153	0.168
40	0.151	0.191	0.159	0.182	0.144	0.165	0.150	0.169	0.156	0.170	0.153	0.167
35	0.160	0.188	0.164	0.180	0.146	0.161	0.152	0.165	0.157	0.170	0.159	0.168
30	0.168	0.185	0.171	0.180	0.150	0.156	0.170	0.174	0.173	0.175	0.165	0.165

[a] Measured at $U_0 = 140$ fps.
[b] Measured at $U_0 = 70$ fps.
[c] Rounded leading and trailing edges.

Table 6 Summary of mean values of calculated Strouhal numbers

Model chord, c, in.	Flow constriction ratio, K	Mean value of Strouhal numbers $-30 \leq \alpha \leq 90$ S^*	S	$-35 \leq \alpha \leq 90$ S^*	S
1.991[a]	3.51	0.154	0.216	0.153	0.219
1.326[a]	5.27	0.148	0.181	0.147	0.183
1.000[a]	6.99	0.149	0.175	0.147	0.175
1.000[b]	6.99	0.149	0.176	0.147	0.176
0.500[a]	13.98	0.149	0.164	0.148	0.164
1.349[a, c]	5.18	0.162	0.197	0.162	0.199

[a] Measured at $U_0 = 140$ fps.
[b] Measured at $U_0 = 70$ fps.
[c] Rounded leading and trailing edges.

Pressure Distribution on an Inclined Plate in a Constricting Flow Channel

In order to provide a more complete description of the average flow over an inclined plate in a constricting flow channel, the static-pressure distribution over the front surface of such a plate was measured as a function of the angle of attack. The measurements were performed on the 1.326-in. flat plate for which $K = 5.27$. This model size was chosen as a compromise; the influence of the flow constriction was strongly felt in $C_p{}^*$ as shown in Fig. 8, and at the same time S^* was essentially the same as that for the two plates of smaller chord.

The pressure was measured at twelve different stations along the chord at each incidence. The incidence was varied in 5-deg increments, from 30 to 90 deg. The techniques used to measure the distribution on such a small model and all of the results are presented in detail in [9].

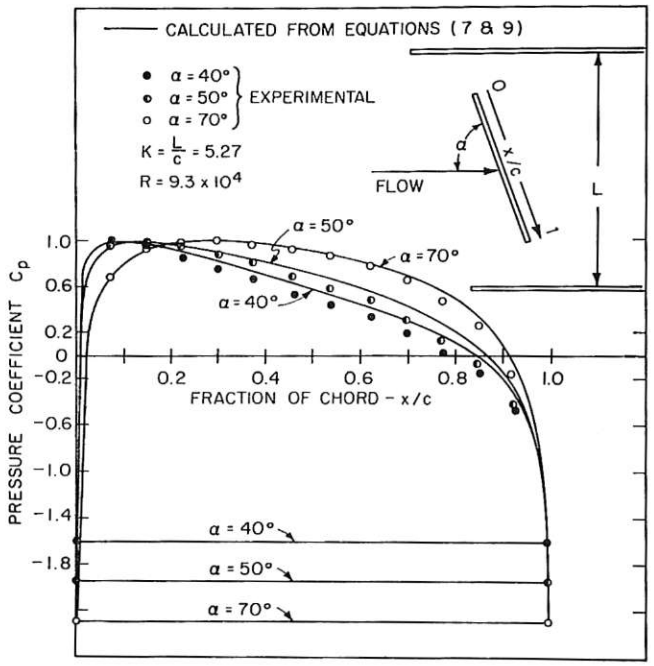

Fig. 9 Calculated and experimental pressure coefficients on inclined sharp-edged plates for $K = 5.27$

The pressure distributions for $\alpha = 40$, 50, and 70 deg are representative of all the data and are shown in Fig. 9. A theoretical pressure distribution for each of these three angles of incidence was calculated, using the modified free-streamline theory derived in this paper, and is plotted in Fig. 9 along with the experimental results. A similar comparison between experiment and theory is shown in Fig. 3 for the case of relatively little ($K = 14$) lateral restriction of the flow field. Comparing the experimental results of Figs. 3 and 9 indicates that constricting the flow influences the pressure distribution primarily in the vicinity of the leading and trailing edges. The free-streamline theory, which was developed for an infinite flow field, quite accurately predicts the pressure distribution for $K = 14$, and even for the case of considerable lateral restriction of the flow ($K = 5.27$) the agreement between this theory and experiment is fair.

Conclusion

The modified free-streamline theory of Roshko has been extended to include an inclined flat plate in an infinite flow field at an arbitrary angle of attack. There is excellent agreement between theory and experiment regarding both pressure distribution and location of the free streamlines for the case of relatively little lateral restriction of flow ($K = 14.0$); the agreement is only fair when the tunnel height is only 5.27 times the model chord.

The mean separation between the free-vortex layers from a sharp-edged flat plate in a bluff-body flow has been found experimentally to be 1.41 $c \sin \alpha$ over a very wide range of lateral constriction of the flow. Using this separation distance as a characteristic dimension of the flow along with the maximum mean speed in the separated vortex layers and the vortex-street frequency, it has been possible to formulate a modified Strouhal number S^* which is essentially independent of both the angle of attack and flow constriction and equal to 0.15.

Since D varies in a known way with α independent of K (from 3.51 to ∞ presumably), and since S^* is equal to a constant for sharp-edged plates, it is possible to calculate the pressure coefficient behind such plates simply from a knowledge of the vortex-street frequency and the angle of attack. If the lateral constriction is not too great ($K > 5.3$), it is further possible to calculate the pressure distribution on the front surface of the plate and the center line of the free-vortex layers from the free-streamline theory presented.

Acknowledgments

This work formed a part of a broad program of research in stall propagation in axial-flow compressors directed by Prof. H. W. Emmons and financially supported by the Pratt & Whitney Aircraft Corporation. The author is indebted to Professor Emmons and other members of the Harvard University faculty for many fruitful discussions.

References

1 H. Lamb, "Hydrodynamics," Dover Publications, New York, N. Y., sixth edition, 1945, pp. 99–103.
2 O. Flachsbart, "Messungen an ebenen und gewolbten Platten," *Ergebnisse der Aerodynamischen Versuchanstalt zu Gottingen*, vol. 4, 1932, pp. 96–100.
3 A. Fage and F. C. Johansen, "On the Flow of Air Behind an Inclined Flat Plate of Infinite Span," *Proceedings of The Royal Society*, London, England, series A, vol. 116, 1927, pp. 170–197.
4 A. Roshko, "A New Hodograph for Free-Streamline Theory," NACA TN 3168, 1954.
5 A. Roshko, "On the Wake and Drag of Bluff Bodies," *Journal of the Aeronautical Sciences*, vol. 22, 1955, pp. 124–132.
6 A. Roshko, "On the Drag and Shedding Frequency of Two-Dimensional Bluff Bodies," NACA TN 3169, 1954.
7 G. K. Batchelor, "A Proposal Concerning Laminar Wakes Behind Bluff Bodies at Large Reynolds Numbers," *Journal of Fluid Mechanics*, vol. 1, 1956, pp. 388–398.
8 A. Fage and F. C. Johansen, "The Structure of the Vortex Sheet," *Philosophical Magazine*, series 7, vol. 5, 1928, pp. 417–441.
9 F. H. Abernathy, "Flow Over an Inclined Plate," PhD thesis, Division of Engineering and Applied Physics, Harvard University, Cambridge, Mass., 1958.
10 L. M. Rose and J. M. Altman, "Low-Speed Investigation of the Stalling of a Thin, Faired, Double Wedge Airfoil With Nose Flat," NACA TN 2172, 1951.